Molecular Mechanics Force Fields for Linear Metallocenes

Thompson N. Doman,[†] Clark R. Landis,*[,‡] and B. Bosnich*[,†]

Contribution from the Department of Chemistry, 5735 South Ellis Avenue, The University of Chicago, Chicago, Illinois 60637, and Department of Chemistry, University of Wisconsin, Madison, Wisconsin 53705. *Received February 14, 1992*

Abstract: A self-consistent molecular mechanics force field for a series of linear metallocenes, $[M(Cp)_2]$ (M = Fe(II), Ru(II), Os(II), V(II), Cr(II), Co(II), Co(III), Fe(III), Ni(II); Cp is the cyclopentadienyl ligand), has been developed. The molecular topology of these π-complexes is defined in terms of a dummy atom located at the centroid of the Cp ligands. The forces and curvature elements which are initially associated with the dummy atoms are eventually transferred to the defining atoms of the ligands. Nearly all of the force constants were derived from vibrational data. It was found that the internal ligand force constants for the Cp ligand were essentially transferrable from metal to metal but that the skeletal force constants involving the metal and the Cp rings were specific for a particular metal. The force constants were found to be capable of reproducing the observed structures to within a few percent in most cases, even in highly strained metallocenes. A number of silicon parameters were derived from vibrational data. These were used to calculate the structure of a metallocene containing a silicon strap. The issue of whether linear metallocenes prefer to adopt a staggered or an eclipsed conformation is addressed by a number of examples. It is concluded that the preference for the eclipsed conformation is almost totally decided by electronic effects and not by nonbonded interactions. The conformations of the methyl groups in decamethylmetallocenes are not reproduced by the force field, and it may be that the methyl group conformations are also decided by electronic effects.

The application of molecular mechanics to the understanding of structure and stability of transition metal complexes has its conceptual roots in the early work of Mathieu[1] and of Bailar and Corey.[2] The former noted that certain chelate ring systems are capable of adopting preferred conformations, and the latter employed these ideas to calculate the nonbonded intra- and interligand interactions of bidentate chelate compounds. With the advent of more sophisticated empirical force fields, minimization techniques, and faster computational methods developed for organic systems,[3] a number of attempts were made to apply these methods to coordination compounds, mainly cobalt(III) amine complexes. The most notable of these attempts was the work of Snow[4] and Hawkins,[5] who developed force constants and employed minimization techniques in order to derive structures and stabilities of diastereomeric cobalt(III) amine complexes. To a large extent the force field parameters were derived empirically to fit known crystal structures, although Snow attempted to connect some force constants to spectroscopic data. All of the subsequent work on coordination compounds is, to a greater to lesser extent, based on these early studies.[6-8] Many refinements were introduced, so that at present, there exists a reliable body of empirical information for deriving the structures of many classical coordination compounds.

Until recently, organometallic compounds of the transition metals have received less attention although various strategies have been adopted in order to assess steric interactions or to obtain approximate structures. Among these were attempts to determine steric interactions by minimizing the van der Waals energy of rotamers while bond distances and angles were held constant.[9,10] A somewhat more sophisticated method has been applied for the same purpose[11,12] using the "Dreiding" force field.[13] The Dreiding force field employs generic force constants based on atom types and is found to reproduce organic crystal structures reasonably well. It promises to be useful for transition metal complexes also.[12] In addition there are a variety of commercial programs which purport to deal with organometallic systems.

One of us has recently reported the development of a force field, SHAPES,[14] based on angular overlap considerations that leads to a general description of the variety of special geometries observed for organometallic complexes. The SHAPES force field was parametrized by ab initio calculations, structure-based optimization, and normal coordinate analysis. Application of this force field to square planar rhodium(I) complexes reproduced the structures well.

This paper is devoted to the development of a spectroscopically based empirical force field for bis-cyclopentadienyl metal complexes of the type $[M(Cp)_2]^{n+}$. These species were chosen because they represent one of the historic pillars of organometallic chemistry and they present the general challenge of embodying π-ligand coordination into empirical force fields.

1. Force Field

For the present study we employed the CHARMM force field[15] and the facilities of the CHEM-X program[16] as the graphics front end. The CHARMM force field was chosen for a variety of reasons, the most important being its ability to derive force constants from experimental vibrational data. Throughout we have tried to use self-consistent spectroscopically based force constants as much as possible. Because of the structural peculiarities of metallocenes, the source code of CHARMM has been modified.

In the force field calculations, the total energy of the molecule in vacuo is given by the sum of contributions from the energy terms associated with bond stretching, angle bending, torsional deformations, nonbonded van der Waals interactions, and electrostatic interactions. No improper torsion terms nor off-diagonal terms such as stretch-bend were used in the present computations. The individual energy terms are defined as follows.

Bond Stretch. The force constant for the bond stretch terms, k_b, is defined by the harmonic potential energy, E_b:

[†] The University of Chicago.
[‡] University of Wisconsin.

(1) Mathieu, J. P. *Ann. Phys. (Paris)* **1944**, *19*, 335.
(2) Corey, E. J.; Bailar, J. C. *J. Am. Chem. Soc.* **1959**, *81*, 2620.
(3) Allinger, N. L.; Burkert, U. *Molecular Mechanics*; American Chemical Society: Washington, DC, 1982.
(4) Snow, M. R. *J. Am. Chem. Soc.* **1970**, *92*, 3610.
(5) Gollogly, J. R.; Hawkins, C. J. *Inorg. Chem.* **1969**, *8*, 1168.
(6) Brubaker, G. R.; Johnson, D. W. *Coord. Chem. Rev.* **1984**, *53*, 1.
(7) Hancock, R. D. *Prog. Inorg. Chem.* **1989**, *37*, 187.
(8) Pozigun, D. V.; Kuz'min, V. E.; Kamalov, G. L. *Russ. Chem. Rev.* **1990**, *59*, 1093.
(9) Bogdan, P. L.; Irwin, J. J.; Bosnich, B. *Organometallics* **1989**, *8*, 1450.
(10) (a) Davies, S. G.; Derome, A. E.; McNally, J. P. *J. Am. Chem. Soc.* **1991**, *113*, 2854. (b) Blackburn, B. K.; Davies, S. G.; Sutton, K. H.; Whittaker, M. *Chem. Soc. Rev.* **1988**, *17*, 147.
(11) Lin, Z.; Marks, T. J. *J. Am. Chem. Soc.* **1990**, *112*, 5515.
(12) Castonguay, L. A.; Rappé, A. K.; Casewit, C. J. *J. Am. Chem. Soc.* **1991**, *113*, 7177.
(13) Mayo, S. L.; Olafson, B. D.; Goddard, W. A. *J. Phys. Chem.* **1990**, *94*, 8897.
(14) Allured, V. S.; Kelly, C. M.; Landis, C. R. *J. Am. Chem. Soc.* **1991**, *113*, 1.
(15) Brooks, R. ; Bruccoleri, R. E.; Olafson, B. D.; States, D. J.; Swaminathan, S.; Karplus, M. *J. Comput. Chem.* **1983**, *4*, 187.
(16) CHEM-X, developed and distributed by Chemical Design Ltd., Oxford, England.

0002-7863/92/1514-7264$03.00/0

$$E_b = \sum_{bonds} k_b(r - r_0)^2$$

where k_b is in kcal/mol·Å^2 and r_0 is the equilibrium bond distance in Å. (Note that the $^1/_2$ usually associated with this term is absorbed into k_b. We adopt this practice throughout.)

Angle Bend. Except for bond angles involving the metal as the central atom, the usual harmonic potential was used:

$$E_\theta = \sum_{angles} k_\theta(\theta - \theta_0)^2$$

where k_θ is the angle bending force constant in kcal/mol·rad^2 and θ_0 is the equilibrium bond angle. The θ_0 values used here are the idealized values expected for the $[M(Cp)_2]$ molecule.

For metal-centered angle bends in metallocenes, we used a Fourier potential truncated at the leading term. The Fourier energy E_F is given by

$$E_F = \sum_{angles} k_F[1 + \cos(n\theta - \delta)]$$

where k_F is the bending force constant, n is the periodicity, θ is the angle, and δ is the phase shift. For the present metallocenes only a single Fourier angle is considered, namely, the ring centroid–metal–ring centroid angle where the appropriate values are $n = 2$ and $\delta = 180°$. The Fourier angle bend function was implemented in CHARMM previously[15] because many organometallic systems exhibit large bond angle distortions which are better described by a Fourier potential than by the usual harmonic approximation. For most of the systems described here, it is probable that a harmonic potential is sufficient to describe metal-centered bends, but we included the Fourier term for reasons of generality. The relationship between the Fourier force constant k_F and the harmonic force constant k_θ is $k_F = 2k_\theta/n^2$ for moderate angle deformations.

Torsion Angles. The energy, E_T, for torsional deformations is given by a similar truncated Fourier expression:

$$E_T = \sum_{torsions} k_T[1 + \cos(n\phi - \delta)]$$

where ϕ is the torsion angle, n is the periodicity, δ is the phase shift, and k_T is one-half of the barrier height (kcal/mol). For $[M(Cp)_2]^{n+}$ complexes, three Cp ring torsion terms were used, namely, the torsions H–C–C–H, H–C–C–C, and C–C–C–C. The equilibrium torsion values were set to maintain planarity of the Cp rings, that is, $n = 2$ and $\delta = 180°$. We modified the CHARMM source code to include a 5-fold torsion term, which was needed to describe Cp rotations about the metal. The equilibrium value of this 5-fold torsion term depends on whether the metallocene prefers to adopt an eclipsed or a staggered conformation. All other possible torsions of $[M(Cp)_2]^{n+}$ were set to zero. Ring substitution can introduce new torsion terms which we discuss when the case arises.

van der Waals Interactions. The nonbonded van der Waals interactions were calculated using the Lennard-Jones 6–12 potential:

$$E_{VDW} = \sum_{i<j} \epsilon_{ij}[(r_0/r_{ij}^{12}) - 2(r_0/r_{ij}^{6})]$$

where ϵ_{ij} is the well depth (kcal/mol), r_0 is the van der Waals "bond" length (Å), and r_{ij} is the internuclear distance of the atoms i and j. The usual assumptions are made, namely, that $r_0 = {}^1/_2(r_i + r_j)$, where r_i and r_j are the van der Waals radii of the atoms i and j, and $\epsilon_{ij} = (\epsilon_{ii}\epsilon_{jj})^{1/2}$, where ϵ_{ii} and ϵ_{jj} are the van der Waals well depths for like interactions. Nonbonded van der Waals interactions are not calculated for 1,2- and 1,3-interactions: these interactions are absorbed into the stretching and bending force constants, respectively.

Except for the metal atoms, the parameters, ϵ_{ij} and r_0 used here are those found in the standard CHARMM parameter list. The van der Waals parameters for the metal atoms were assigned the values $\epsilon = 0.001$ kcal/mol and $r_0 = 1.0$ Å for all metals. The choice of these parameters is arbitrary, but the minimized structures are not greatly affected by the values of these parameters within reasonable limits. Thus, for the present systems, increasing r_0 to 2 Å and ϵ to 0.1 kcal/mol caused a slight change in the total energy but no significant change in structural parameters. Similarly, reducing the values of these parameters had little effect on the energy or structure. Thus, it seems that the results described here are not very sensitive to the choice of metal van der Waals parameters.

Electrostatic Interactions. For the electrostatic interaction contribution to the total energy, we used an attenuated form of the potential energy in keeping with the practice of CHARMM and other force fields. The attenuated form of the potential assumes a distance-dependent dielectric constant of the form $\epsilon_0 = \epsilon' r_{ij}$, where ϵ_0 is the dielectric constant, ϵ' is a proportionality constant and is set to 1, and r_{ij} is the distance between the ith and jth atoms bearing the charges q_i and q_j, respectively. The energy E_E in kcal/mol of the attenuated electrostatic potential is then given by

$$E_E = \sum_{i<j} q_i q_j / 4\pi\epsilon_0 r_{ij}$$

We found that the attenuated form of the potential gave better structural reproducibility than did the classical form. The partial charges were calculated by the "charge equilibration" method,[17] which depends on the experimental atomic ionization potentials, electron affinities, and radii. This method allows for the calculation of partial charges on all atoms including the metal. Since these calculations depend on geometry, the partial charges were recalculated after every 50 iterations of the minimization cycle. It was found that, when the molecule approached the minimized structure, little change in the partial charges was observed. We found that the inclusion of charges caused small geometric changes in the minimized structures, but charges made a substantial contribution to the total energy. As for the van der Waals interactions, electrostatic energies associated with 1,2- and 1,3-interactions were not included.

In all of these calculations, we aimed for minimized structures which reproduced experimental bond lengths to ±0.02 Å and bond angles to ±3° in the majority of cases. Since nearly all of the experimental structural data is derived from X-ray diffraction of crystals, variations in bond length and angle of this magnitude could well be accounted for by the exigencies of crystal packing.

2. Vibrational Analysis

The molecular mechanics force constants used here were largely derived from the vibrational data of the parent molecules. There were cases where, for various reasons, the parameters were fitted to structural data, but even for the derivation of these constants the vibrational analysis was useful.

The molecular mechanics force constants were derived from experimental vibrational data in the follow way. First, a set of Cartesian coordinates for the molecule was input. The input structure is usually derived from X-ray diffraction although, in principle, any reasonable structure will suffice. Second, a list of molecular mechanics force constants and van der Waals parameters is input. The values of these force constants are usually educated guesses based on analogous molecules. Third, using this set of initial parameters the structure is energy minimized. We used the adopted basis set Newton–Raphson minimizer routine.[15] Fourth, a vibrational analysis is then performed on the minimized structure. This uses the mass-weighted form of the second derivative matrix of the potential. Diagonalization gives the normal modes and their frequencies. Fifth, the potential energy distribution[18] is calculated for each of the normal modes. This serves to identify the potential energy contribution of each internal coordinate displacement to the total potential energy of each mode. In essence, the potential energy distribution assigns the amount that each mode is constituted of stretch, bend, or torsion displacements. In addition to aiding in assignments, the potential energy distribution serves as a guide to the adjustment of force constants to match the experimental frequencies.

At this stage the calculated and observed frequencies are compared, adjustments to the force constants are made, and the process is repeated until a satisfactory set of parameters is obtained

(17) Rappé, A. K.; Goddard, W. A. *J. Phys. Chem.* **1991**, *95*, 3358.
(18) Morino, Y.; Kuchitsu, K. *J. Chem. Phys.* **1952**, *20*, 1809.

which matches the observed frequencies. Usually we aimed for a rms deviation of ±30 cm^{-1} for the observed and calculated frequencies. Although the procedure is routine, if somewhat tedious, it is not always possible to get a good correlation between observed and calculated frequencies for all modes.

3. Definition of Topology

As with all π-complex molecules, the metallocenes of the type $[M(Cp)_2]$ present unique problems in defining the topology for molecular mechanics calculations. Thus, considering the example of ethylene π-bound to a metal, one is presented with a number of alternatives. Do we define the topology in terms of two bonds, one to each of the ethylene carbon atoms, or do we make one (hypothetical) bond to the centroid of the bound olefin? Similarly, in the case of ferrocene, do we define a 10-bond system to the carbon atoms, do we define a linear 2-bond topology defined by the two ring centroids, or do we adopt some other defintion? Ultimately, whatever definition we choose to adopt must apply to all π-bonded systems, and the force field should apply to the atoms involved in bonding and not to some contrived entity such as a centroid.

For the present metallocenes, we considered three alternative topological constructions. First, the topology of the metallocenes could be defined by constructing 10 metal–ligand bonds, one to each of the 10 carbon atoms of the two Cp rings. Whereas such a topology may bear a resemblance to the actual bonding, the implementation of such a topology for molecular mechanics calculations presents formidable problems, not the least of which is the fact that a succession of fully contiguous 3-membered rings is formed, so that any skeletal movements of the Cp ring with respect to each other and with respect to the metal would involve interdependent angle and bond length changes.

Second, we could define a topology which involved a bonded dummy atom at the centroids of the Cp rings. In this construction the dummy atom would have one bond to the metal and five bonds to the carbon atoms of the Cp ring. These bonds would then be assigned force constants for the appropriate stretch, angle, and torsion deformations. Such a scheme is easy to implement, and with the correct force constants, the structures can be reproduced. But this bonded dummy atom scheme is clearly artificial, since bonds do not exist between the dummy atom and the other atoms. Even if this is ignored, the bonded dummy atom method leads to other artifacts. Among these are the large force constants required to maintain the dummy atom at the centroid position and the introduction of nonexistent vibrational modes arising from the artificial bonds that are introduced. Hence appropriate force constants cannot be derived from this topological definition, and the method does not realistically describe the forces that apply to the molecule.

The third topological definition resembles the dummy atom scheme but is devoid of its problems and is capable of realisitically representing the forces which operate in a π-complex. We adopt this scheme here and we refer to it as the "dummy atom topology". In this topological definition the dummy atom is a massless geometrical entity, the coordinates of which are specified by the defining atoms of the π-ligand. In the case of the Cp ligand the dummy atom position would be defined by the five carbon atoms of the ring, and for the Cp ligand itself, it would be placed at the centroid of the ring. If, however, there are reasons for believing that the dummy atom should not lie at the centroid, then it can be placed off-center according to the perceived bonding of the π-ligand to the metal. For example, in the case of an unsymmetrically substituted Cp, it may be considered more realistic to place the dummy atom in an off-center position. For all of the systems discussed here, the dummy atom was placed at the centroid of the five defining atoms.

In this dummy atom construction, we initially assign force constants to the metal–dummy stretch, the metal–dummy–(Cp) carbon bends, and so on. Although these force constants are initially applied in this way, all of the forces associated with the dummy atom are eventually distributed among the defining atoms of the molecule, leaving no forces on the dummy atom. During minimization, the dummy atom position is continually recalculated. This scheme, in effect, uses the simple topology of the dummy atom but in the end applies the forces to appropriate entities, namely, the defining atoms of the molecule. This method has the advantage of allowing for the vibrational analysis of the molecule. The details for the implementation of this scheme are described elsewhere.[19] We note that a similar force distribution method has been applied in a different context.[20] We illustrate the essential features with the simplest example of an ethylene π-complex.

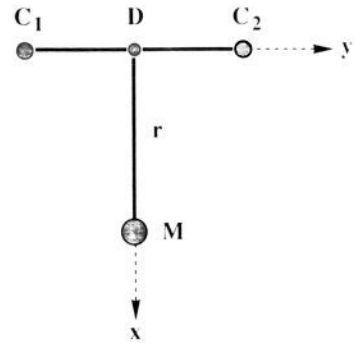

Figure 1. Coordinate frame for an η^2-ethylene bound to a metal.

For the minimization procedure and the vibrational analysis the first and second derivatives of the energy E are required. To illustrate how the forces are distributed from the dummy atom to the defining atoms, we consider the metal–ligand stretch for a hypothetical metal–π-ethylene complex only for the x-coordinate. The topology is shown in Figure 1.

Placing the dummy atom, D, at the centroid between C_1 and C_2 carbon atoms of the bound ethylene, the x-coordinate of the dummy atom X_D is related to the x-coordinates of the carbon atoms X_{C1} and X_{C2} by

$$X_D = (X_{C1} + X_{C2})/2$$

and

$$r = X_D - X_M$$

where X_M is the x-coordinate of the metal, M. The energy, E, for the metal–dummy stretch is given by

$$E = k_S(r - r_0)^2$$

and

$$\partial E/\partial r = 2k_s(r - r_0)$$

By the chain rule, the force on the dummy atom is

$$\partial E/\partial X_D = (\partial E/\partial r)(\partial r/\partial X_D) = [2k_s(r - r_0)][1] = 2k_s(r - r_0)$$

The force on the dummy atom can be passed to C_1 by the chain rule relationship:

$$\partial E/\partial X_{C1} = (\partial E/\partial X_D)(\partial X_D/\partial X_{C1}) = [2k_s(r - r_0)][1/2]$$

Thus, in this simple example, one-half of the force on the dummy atom is passed on to C_1. It is obvious that, in a similar way, the other one-half of the force can be passed on to C_2. The result is that the two defining atoms C_1 and C_2 carry the force and no forces remain on the dummy atom. It is clear that this procedure can be extended to more complex systems and cases where the dummy atom is not placed at the centroid. Moreover, the second derivatives needed for the vibrational analysis can also be distributed among the defining atoms by applications of the chain rule. The angle terms can be dealt with in a similar manner.

(19) Doman, T. N.; Landis, C. R. *J. Comput. Chem.*, submitted for publication.

(20) van Gunsteren, W. F.; Boelens, R.; Kaptein, R.; Scheek, R. M.; Zuiderwig, E. R. P. In *Molecular Dynamics and Protein Structure*; Hermans, J., Ed.; Polycrystal Book Service: West Springs, IL, 1985; p 92.

Table I. Molecular Mechanics Vibrational Analysis of Ferrocene

freq no.	rep	frequencies (cm^{-1}) obsd	calcd	dev
6	A_{1u}	44	42	−2
22	E_{1u}	179	177	−2
4	A_{1g}	309	282	−27
16	E_{1g}	389	363	−26
11	A_{2u}	478	493	15
21	E_{1u}	492	498	6
34	E_{2u}	569	591	22
28	E_{2g}	597	594	−3
2	A_{1g}	814	742	−72
9	A_{2u}	820	742	−78
14	E_{1g}	844	920	76
19	E_{1u}	855	924	69
33	E_{2u}	885	806	−79
27	E_{2g}	897	806	−91
13	E_{1g}	998	999	1
18	E_{1u}	1005	1000	−5
31	E_{2u}	1055	979	−76
25	E_{2g}	1058	979	−79
3	A_{1g}	1102	999	−103
10	A_{2u}	1110	999	−111
30	E_{2u}	1189	1071	−118
24	E_{2g}	1191	1071	−120
7	A_{2g}	1250	1253	3
5	A_{1u}	1255	1253	−2
32	E_{2u}	1351	1477	126
26	E_{2g}	1356	1477	121
15	E_{1g}	1410	1576	166
20	E_{1u}	1410	1576	166
17	E_{1u}	3077	3103	26
29	E_{2u}	3085	3104	19
12	E_{1g}	3086	3103	17
23	E_{2g}	3100	3104	4
8	A_{2u}	3103	3107	4
1	A_{1g}	3110	3107	−3

4. Force Constants of Ferrocene

Extensive vibrational data and spectroscopic assignments for the alkali metal salts, CpM,[21-23] and for the $[Fe(Cp)_2]$ and $[Ru(Cp)_2]$ complexes[24] are available. Data for the other linear metallocenes are less comprehensive. It is convenient to divide the force constants for the linear metallocenes into those associated with the internal ligand vibrations and those associated with the skeletal modes involving the metal and the ligands.

It was important to establish whether the molecular mechanics force constants associated with the internal ligand modes were transferable from metal to metal. The vibrational frequencies observed for the alkali metal salts of Cp both in solids and in solutions are similar; no large frequency shifts are observed.[21-23] This implies that the associated force constants are insensitive to the environment of the Cp ion. As we will discuss presently, we have performed a complete vibrational analysis of ferrocene and have derived the force constants for the internal ligand modes of the bound Cp ligand. Using these force constants we were able to reproduce the observed frequencies reported for CpK[23] reasonably well. Although minor changes in the force constants gave a better fit for the observed frequencies, we found that using these CpK force constants or those derived from ferrocene did not have a significant effect on the minimized energies or structures of linear metallocenes. Two further observations support the notion that the internal ligand force constants are transferable. A full molecular mechanics vibrational analysis of $[Ru(Cp)_2]$ reveals that the internal ligand force constants are essentially unaltered from those obtained for $[Fe(Cp)_2]$. The transferability of force constants for the internal ligand modes of CpK and $[Fe(Cp)_2]$ has been demonstrated by a conventional normal coordinate analysis of the vibrational spectra of the two species.[25] Thus the assertion that the internal ligand force constants are essentially transferable seems secure, and we use the internal ligand force constants derived for $[Fe(Cp)_2]$ for all of the linear metallocenes discussed here.

The results of the vibrational analysis of ferrocene are shown in Table I. Included in this table are the conventional frequency numbering[24] and their respective assignments[24] based on the D_{5d} point group representing the staggered conformation of ferrocene. The symmetry labels change, but the analysis is not dependent on whether the D_{5d} or the eclipsed conformation D_{5h} point group

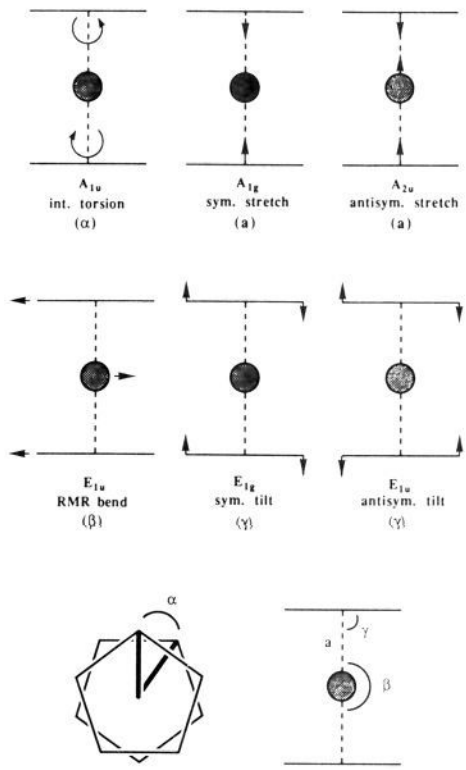

Figure 2. Representation of the skeletal modes of a linear metallocene. The Cp rings are represented by horizontal lines and the metal by a dark circle. The 1,5-dihedral angle, α, the M–D stretch, a, the D–M–D bend, β, and the C–D–M bend, γ, are shown.

Table II. Skeletal Force Constants Derived for Ferrocene

term[a]	force const	equilibrium value
Fe–D (stretch) (kcal/mol·Å²)	205	1.649 Å
Fe–D–C (bend) (kcal/mol·rad²)	100	90°
D–Fe–D (bend) (kcal/mol·rad²)	40	*n*, 2; δ, 180°
1,5-dihedral (kcal/mol)	0.36	*n*, 5; δ, 180°

[a] D is the dummy atom.

Table III. Internal Cyclopentadienyl Force Constants

term	force const[a]	equilibrium value
C–C (stretch)	400	1.42 Å
C–H (stretch)	375	1.08 Å
C–C–C (bend)	100	108°
C–C–H (bend)	30	126°
C–C–C–C (torsion)	6	*n*, 2; δ, 180°
C–C–C–H (torsion)	4	*n*, 2; δ, 180°
H–C–C–H (torsion)	1.5	*n*, 2; δ, 180°

[a] The units for these force constants are those defined earlier.

(21) Fritz, H. P. *Adv. Organomet. Chem.* **1964**, *1*, 239.
(22) Fritz, H. P.; Schäfer, L. *Chem. Ber.* **1964**, *97*, 1829.
(23) Garkusha, O. G.; Garbuzova, I. A.; Lokshin, B. V.; Mink, J. *J. Mol. Struct.* **1988**, *175*, 165.
(24) Bodenheimer, J. S.; Low, W. *Spectrochim. Acta* **1973**, *29A*, 1733.
(25) Brunvoll, J.; Cyvin, S. J.; Schäfer, L. *J. Organomet. Chem.* **1971**, *27*, 107.

is chosen. The calculated and observed frequencies are listed together with the deviations. The overall rms deviation is about 75 cm^{-1}, which is somewhat larger than we would have preferred. Given, however, that 34 frequencies are fitted and an approximate force field is used, the fit is good.

The first six frequencies listed in Table I are associated with the skeletal modes of ferrocene. They are depicted in Figure 2, and the force constants derived from the vibrational analysis are listed in Table II. The equilibrium value for the metal–Cp centroid distance was taken from neutron diffraction data.[26] Force constants for the internal modes of the bound Cp ligand are listed in Table III. The equilibrium bond distances, bond angles, and torsion angles are representative of those found for numerous structures of linear metallocenes. Before we describe our results from the molecular mechanics calculations on ferrocene, we address a long-standing issue concerning the conformation of ferrocene.

5. Equilibrium Conformation of Ferrocene

The ferrocene molecule could exist in an eclipsed, staggered, or some intermediate conformation. In the solid state the structure is disordered at ambient temperatures probably because of rotation of the Cp rings.[27] At low temperatures, where Cp rotation is retarded, both X-ray[28] and neutron[26,29] diffraction data indicate that the structure remains disordered and the rings are staggered by about 10°. Electron diffraction data in the gas phase,[29] however, suggest that the ferrocene molecule prefers to adopt an eclipsed conformation with an internal rotational barrier of 0.9 (3) kcal/mol. On the basis of these data it seems that ferrocene prefers to adopt and eclipsed conformation with a low internal rotational barrier. A theoretical rationalization has been provided for this preference.[30]

Considering the skeletal vibrations illustrated in Figure 2, we note that the A_{1u} torsion represents internal rotation of the rings. To describe this internal rotation, we define a single 1,5-dihedral angle by the angle (α, Figure 2) that is formed by the connections between a carbon atom of one Cp ring to its dummy atom, then to the dummy atom of the other Cp ring, and finally, to a carbon atom of the second Cp ring. It is referred to as a 1,5-dihedral term because of the 1,5-connectivity of the two carbon atoms, namely, the connectivity carbon–dummy–metal–dummy–carbon. Hence, by knowing the force constant for this 1,5-dihedral term, we should be able to determine the barrier height. The A_{1u} vibration was found to occur at 44 cm^{-1} by vibrational spectroscopy at 80 K;[31] a slightly higher value of 50 cm^{-1} was found by inelastic neutron scattering.[32] We derive a molecular mechanics force constant, k, for this dihedral term of 0.36 kcal/mol (Table II). The dihedral energy term can be rewritten in the form

$$E = k[1 - \cos(n(\alpha - \alpha_0))]$$

where E is the energy, k is the torsional force constant, n is the periodicity, α is the angle, and α_0 is the equilibrium angle. We assume that we can describe the barrier height as

$$\Delta E = E_{max} - E_{min} = k\{[1 - \cos(5(36-0))] - [1 - \cos(5(0-0))]\}$$

The barrier height, ΔE, for the 5-fold rotation has a maximum at 36° and a minimum at 0°. Thus,

$$\Delta E = 2k = 0.72 \text{ kcal/mol}$$

Table IV. Molecular Mechanics Energy Terms of the Eclipsed and Staggered Conformations of Ferrocene

	energy (kcal/mol)	
term	eclipsed	staggered
bond	0.079	0.073
angle	0.000	0.000
dihedral	0.004	0.724
van der Waals	−5.225	−5.251
electrostatic	13.766	13.775
total	8.625	9.321

which is similar to the value found from gas-phase electron diffraction. This force constant k was used in the molecular mechanics calculations.

6. Structure of Ferrocene

It should be recognized that the calculated, minimized structure of ferrocene is bound to correspond to the observed structure because the process of deriving the force constants by matching vibrational data involves a minimization process. Nonetheless, certain features in the minimized structure arise from secondary consequences. As expected, all of the bond lengths, bond angles, and torsions are reproduced to within a few percent. If the 1,5-dihedral term is not included, the minimized structure has a prefectly staggered conformation (α = 36°). Inclusion of this term produces a perfectly eclipsed conformation (α = 0). Perhaps the most interesting feature of the minimized structure is the energy distribution among various molecular mechanics energy terms. The calculated energies for the eclipsed and staggered conformations are given in Table IV. It will be noted that the individual energy contributions are essentially the same for all entries except that for the dihedral term. Two counterintuitive facts emerge. First, the van der Waals and electrostatic contributions are essentially the same for the staggered and for the eclipsed conformers. Second, the van der Waals contributions are attractive in both cases and not repulsive, as was commonly supposed. The fact that all terms, except the dihedral term, are essentially the same indicates that the preference for the eclipsed conformation arises solely from the 1,5-dihedral term; the calculated barrier of 0.72 kcal/mol appears in the dihedral term of the staggered conformation (Table IV). Thus we may draw the important conclusion that the preference for the eclipsed conformation of ferrocene arises not from any nonbonded interactions but is probably caused by electronic effects. This is an interesting result because it was long assumed that the conformation of ferrocene was somehow connected with nonbonded interactions.

Finally, we note that the hydrogen atoms of the Cp rings were found to tilt slightly toward the metal (1.6 (4)°).[26,29] We find that the attractive van der Waals interactions cause a small inward tilt of the hydrogen atoms but that the larger repulsive electrostatic interactions lead to a net tilt of the hydrogen atoms away from the metal (0.24°). This effect can also be traced to an electronic origin.[33]

7. Ruthenocene and Osmocene

The crystal structures of ruthenocene,[34] and osmocene[35] have been determined although little data was provided for the latter. Both molecules exist in the eclipsed form. A full vibrational analysis of ruthenocene is available,[24] and a partial analysis is available for osmocene.[36] From these data we were able to derive skeletal force constants by matching the calculated frequencies with those observed for particular modes. In both cases the agreement was excellent: the rms deviation for ruthenocene was 28 cm^{-1} and for osmocene it was 31 cm^{-1}. The published data allowed us to determine the barrier height for the internal (1,5-

(26) Takusagawa, F.; Koetzle, T. F. *Acta Crystallogr.* **1979**, *B35*, 1074.
(27) Edwards, J. W.; Kington, G. L.; Mason, R. *Trans. Faraday Soc.* **1959**, *55*, 660.
(28) (a) Seiler, P.; Dunitz, J. D. *Acta Crystallogr., Sect. B.* **1979**, *35*, 2020. (b) Seiler, P.; Dunitz, J. D. *Acta Crystallogr., Sect. B.* **1979**, *35*, 1068.
(29) Haaland, A. *Acc. Chem. Res.* **1979**, *12*, 415 and references therein.
(30) Carter, S.; Murrell, J. N. *Organomet. Chem.* **1980**, *192*, 399.
(31) Rocquet, F.; Berreby, L.; Marsault, J. P. *Spectrochim. Acta* **1973**, *29A*, 1101.
(32) Gardner, A. B.; Howard, J.; Richardson, R.; Tomkinson, J.; Waddington, T. C. ILL (Grenoble) Report No. 09-03-224, 1980. Referenced by Chlor, K.; Lucazeau, G.; Sourisseau, C. J. *Raman Spectrosc.* **1981**, *11*, 183.
(33) Elian, M.; Chen, M. M. L.; Mingos, M. P.; Hoffmann, R. *Inorg. Chem.* **1976**, *15*, 1148.
(34) Seiler, P.; Dunitz, J. D. *Acta Crystallog.* **1980**, *B36*, 2946.
(35) Jellinek, V. F. *Naturforsch. B* **1959**, *14*, 737.
(36) Lokshin, B. V.; Aleksanian, V. T.; Rusach, E. B. *J. Organomet. Chem.* **1975**, *86*, 253.

Table V. Skeletal Force Constants Derived for Ruthenocene and Osmocene

	force constant		equilibrium value	
term[a]	$[RuCp_2]$	$[OsCp_2]$	$[RuCp_2]$	$[OsCp_2]$
M–D (stretch) (kcal/mol·Å²)	205	206	1.816 Å	1.855 Å
M–D–C (bend) (kcal/mol·rad²)	125	130	90°	90°
D–M–D (bend) (kcal/mol·rad²)	52	56	*n*, 2; δ, 180°	*n*, 2; δ, 180°
1,5-dihedral (kcal/mol)	3.4	(3.4)	*n*, 5; δ, 180°	*n*, 5; δ, 180°

[a] D is the dummy atom.

dihedral) rotational barrier for ruthenocene as 6.8 kcal/mol on the basis of the vibration which occurs at 130.8 cm^{-1}. From a thermal motion analysis of the ruthenocene crystal,[34] a barrier height for internal rotation was found to be about 8.1 kcal/mol. This is in good agreement with our vibrationally based value. Both values are based on data from crystals, and the barrier heights may be high because of correlated motion. We have not been able to find reliable data to calculate the internal rotation barrier for osmocene. We suspect it will be larger, but in the force field minimization we have used the ruthenocene value for osmocene.

The derived force constants for the skeletal modes of ruthenocene and osmocene are given in Table V. Comparing these parameters with those of ferrocene (Table II), we note the following. The stretching force constant is about the same for ferrocene and ruthenocene but increases for osmocene. The tilting force constants (M–dummy–C, bend) increase in going down the periodic table. The metal-centered bend force constants also increase in a similar way. In both of the last two cases, the tilts and metal-centered bends, the ruthenocene and osmocene parameters are similar. The derived force constants for the internal ligand modes of ruthenocene were the same as those calculated for ferrocene.

As was found for ferrocene, the derived force constants reproduce the observed ruthenocene and osmocene structures to within a few percent, and all of the driving force to the eclipsed structure can be traced to the 1,5-dihedral term and not to nonbonded interactions.

The nonbonded interactions for ferrocene (Table IV), ruthenocene, and osmocene present an interesting pattern. The van der Waals interactions for the three complexes are −5.22, −4.62, and −4.46 kcal/mol, respectively. Since we have used the same van der Waals parameters for the three metals, the decreasing attraction in going down the periodic table undoubtedly reflects the increase in metal–ligand bond lengths (Os > Ru > Fe). The electrostatic interactions, however, show an unexpected variation. We find that the electrostatic interactions for ferrocene (Table IV), ruthenocene, and osmocene are 13.766, 9.05, and −0.206 kcal/mol, respectively. The charges found on the metals are Fe (+0.446), Ru (+0.301), and Os (−0.0295). In all cases the carbons are δ− and the hydrogens are δ+ in the Cp rings. The disposition of the hydrogen atoms with respect to the ring plane will depend on the appropriate torsion term, the van der Waals interactions, and the electrostatic interactions. In all three molecules, the torsional terms within the Cp rings are the same and the van der Waals interactions are attractive; hence, whether the hydrogen atoms lie above or below the Cp plane will depend on the electrostatic term and on electronic factors not included in these calculations. As we have noted, the hydrogen atoms are by calculation displaced slightly from the Cp plane away from the metal in $[Fe(Cp)_2]$. This is also found for $[Ru(Cp)_2]$ (0.14°), but for $[Os(Cp)_2]$, we find that the hydrogen atoms tilt toward the metal by 0.29°. This last effect we ascribe to the electrostatic attraction of the δ+ hydrogen atoms to the negatively charged osmium atom. We note that these are small effects which depend on the uncertainties associated with the torsion, van der Waals, and electrostatic parameters, but the results serve to illustrate that hydrogen atom tilting can have its partial origin in molecular mechanics.

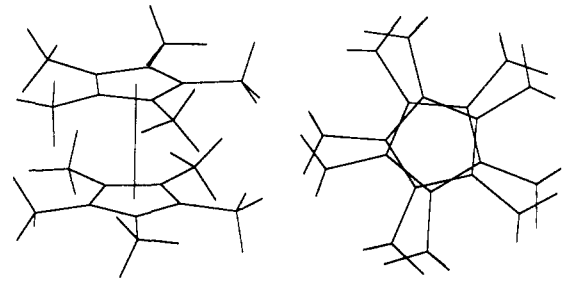

Figure 3. Two perspectives of the minimized structure of $[Fe((CH_3)_5Cp)_2]$ showing the stagger and the orientations of the methyl groups. The top Cp ring has the methyl groups arranged head-to-tail clockwise, the other ring has the methyl groups arranged head-to-tail anticlockwise.

8. Substituted Ferrocenes, Ruthenocenes, and Osmocenes

In this and the following section, we address one of the essential premises of molecular mechanics, namely, the transferability of force constants. Initially we consider the structures of the following molecules: $[Fe((CH_3)_5Cp)_2]$, $[Fe((CH_3)_4Cp)_2]$, $[Ru((CH_3)_5Cp)_2]$, $[Ru((Cl)_5Cp)_2]$, and $[Os((CH_3)_5Cp)_2]$. An accurate crystal structure of $[Fe((CH_3)_5Cp_2)]$ has been determined,[37] and a gas-phase electron diffraction study has been reported.[38] The X-ray diffraction study indicates that the molecule is in a staggered conformation and that the methyl groups are tilted 0.06 Å above the Cp plane away from the metal. The conformation of six of the methyl groups (three on each Cp ring) is such that one hydrogen of each methyl group lies perpendicular to the mean Cp plane away from the metal. The other methyl groups have one of the hydrogen atoms lying nearly parallel to the Cp plane. Using this structural model, the gas-phase electron diffraction results gave an internal rotational barrier of 1 kcal/mol.[38] The $[Fe((CH_3)_4Cp)_2]$ crystal structure[39] is also staggered, and all of the methyl groups are oriented with one hydrogen lying perpendicular to the Cp plane away from the metal. The Cp hydrogen atoms of the two Cp rings lie "trans" ($\alpha = 180°$). A preliminary crystal structure of $[Ru((Cl)_5Cp)_2]$ indicates that the molecule exists in an eclipsed conformation.[40] The chlorine atoms tilt about 0.1 Å from the Cp plane away from the metal. The X-ray diffraction study of $[Ru((CH_3)_5Cp)_2]$ and $[Os((CH_3)_5Cp)_2]$ indicates that the structure is disordered.[41] Although both structures were refined assuming eclipsed conformations, it was recognized that this may be an average structure representing semistaggered conformations. The hydrogen atoms were not located.

For the molecular mechanics minimization, we used the Cp and skeletal force constants derived here for the $[M(Cp)_2]$ species. The inclusion of methyl groups required extra parameters, and the ones we used were the standard organic parameters listed in CHARMM. The only new parameters were the torsion constants for C1–C–C–C1 and C1–C–C–C, both of which were assigned the value 1.0 kcal/mol. (The torsion parameters in CHARMM are generic and are likely to be too "stiff".)

We find the global minimum of $[Fe((CH_3)_5Cp)_2]$ to be a structure having a staggered conformation of $\alpha = 18°$ and not the crystallographically found perfectly staggered angle of 36°. All of the bond lengths and angles are within a few percent of the X-ray structure except for the "gearing" of the methyl groups. In the minimized structure the methyl groups tilt away from the metal by 0.044 Å from the Cp plane compared to 0.06 Å found in the crystal structure. The minimized structure is shown in

(37) Freyberg, D. P.; Robbins, J. L.; Raymond, K. N.; Smart, J. C. *J. Am. Chem. Soc.* **1979**, *101*, 892.
(38) Almenningen, A.; Haaland, A.; Samdal, S.; Brunvoll, J.; Robbins, J. L.; Smart, J. C. *J. Organomet. Chem.* **1979**, *173*, 293.
(39) Schmitz, D.; Fleischhauer, J.; Meier, U.; Schleker, W.; Schmitt, G. *J. Organomet. Chem.* **1981**, *205*, 381.
(40) Brown, G. M.; Hedberg, F. L.; Rosenberg, H. *J. Chem. Soc., Chem. Commun.* **1972**, 5.
(41) Albers, M. O.; Liles, D. C.; Robinson, D. J.; Shaver, A.; Singleton, E.; Wiege, M. B.; Boeyens, J. C. A.; Levendis, D. C. *Organometallics* **1986**, *5*, 2321.

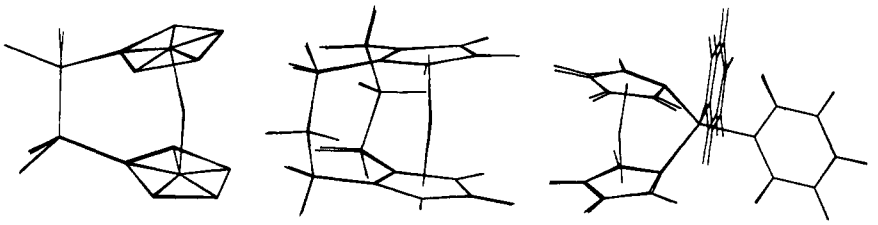

Figure 4. Superimposed calculated and observed structures of the strapped ferrocenes **1**–**3**. The hydrogen atoms in the crystal structure of **1** were not located.

Figure 3, where it will be seen that the methyl group hydrogen atoms have one hydrogen lying approximately in the plane of the Cp ring and the other two hydrogens roughly bisected by the ring plane. Further, if this head-to-tail arrangement is clockwise for one ring, it is anticlockwise for the other. In order to investigate the effect of methyl group conformation on the stagger, we performed a variety of minimizations which enforced different methyl group conformations. Minimization of the conformation where the head-to-tail geared methyl group follows the same direction on both rings leads to a perfectly staggered conformation of the Cp rings ($\alpha = 36°$), but the structure is of higher energy by 0.78 kcal/mol. When the methyl groups were constrained to their crystal structure conformations, the calculated structure had a stagger of 23.7° but the energy was about 5.4 kcal/mol higher than the global minimum. Although a cluster of conformational minima for $[Fe((CH_3)_5Cp)_2]$ may exist around the global minimum because of the interplay between the stagger angle and the orientations of the methyl groups, the structure found in the crystal seems to be too high in energy to be accounted for by the imprecision of molecular mechanics. The difference between the crystal structure and the calculated structure could arise either from crystal packing effects or from electronic effects. It may be that methylated Cp rings require a torsion term to account for the particular orientation found in the structures. We should point out that the 3-fold torsion term used for the methyl groups has no net energy periodicity, so that the methyl group orientations are solely determined by nonbonded interactions. This is the standard formulation for methylated benzene.

In an attempt to resolve the origin of the orientations of the methyl groups that are observed in the crystal but are not reproduced by the isolated molecular calculations, we investigated the effects of crystal packing. In the crystal, all of the $[Fe((CH_3)_5Cp)_2]$ molecules are in identical crystallographic sites, and we considered the effect on one molecule by its 14 nearest neighbors. These 14 neighbors fully envelop the selected molecule, and the distance from the selected molecule's iron atom to the furthest atom of the neighbors is 13.7 Å. We fixed the internal and external coordinates of the neighboring molecules but allowed the internal and external coordinates of the selected molecule to change. For technical reasons we set the electrostatic charges on the atoms of the 14 neighbors to those calculated for the free molecule.

Upon minimization of the crystallographic geometry of the selected molecule, the external coordinates of this molecule did not change but the internal coordinates did. The methyl groups become orientated in a head-to-tail clockwise–clockwise conformation and the Cp rings are perfectly staggered. Other bond lengths and angles are essentially unchanged. It will be recalled that this conformation was found to be slightly higher in energy for the free molecule, which adopted a head-to-tail clockwise–anticlockwise semistaggered conformation. We find that the energy of the crystallographically found orientation of the methyl groups in the observed perfect stagger is nearly 5 kcal/mol higher than that of the head-to-tail clockwise–clockwise structure. Thus crystal packing does appear to have an effect on the conformations of the methyl groups, but it does not cause them to adopt the crystallographically found arrangement. We are therefore constrained to conclude that the methyl groups directly bonded to a coordinated Cp ring require a torsional term which will drive one hydrogen atom to lie perpendicular to the plane of the Cp ring. Perhaps a hyperconjugative effect is involved.

Table VI. Spectroscopically Derived Molecular Mechanics Force Constants and Equilibrium Values for Silicon Compounds[a]

deformation	force const[b]	equilibrium value
	Stretch	
$Si–C_t$	220	1.888 Å
$Si–C_b$	250	1.87 Å
$Si–C_{Cp}$	250	1.87 Å
Si–H	193	1.489 Å
	Bend	
$C_t–Si–C_t$	40	109.5°
$Si–C_t–H$	34	109.5°
$Si–C_t–C_t$	40	109.5°
$C_b–Si–C_b$	60	109.5°
$Si–C_b–C_b$	40	120°
H–Si–H	29	109.5°
$C_b–Si–H$	50	109.5°
$C_b–Si–C_t$	35	109.5°
$Si–C_{Cp}–C_{Cp}$	40	126°
$C_{Cp}–Si–C_b$	60	109.5°
$C_{Cp}–Si–C_{Cp}$	60	109.5°
	Torsion	
$Si–C_b–C_b–H$	3.0	n, 2; δ, 180°
$Si–C_b–C_b–C_b$	3.0	n, 2; δ, 180°
$Si–C_{Cp}–C_{Cp}–H$	3.0	n, 2; δ, 180°
$Si–C_{Cp}–C_{Cp}–C_{Cp}$	3.0	n, 2; δ, 180°

[a] The symbols have the following meanings: C_t is a tetrahedral carbon atom, C_b is a carbon atom of a benzene ring, and C_{Cp} is a carbon atom of a cyclopentadienyl ring. [b] The units of the force constants are those defined earlier.

Table VII. Selected Calculated and Observed Distances and Angles for the Three Strapped Ferrocenes

geometric feature	calcd	found
Tetramethylethyleneferrocene **1**		
Fe–ring distance	1.628 Å	1.631, 1.639 Å
Cp ring tilt angle	19.72°	23°
dummy–iron–dummy angle	167.51°	163.35°
ring stagger	10.64°	9°
strap stagger	23.24°	26°
exocyclic angle ($D–C_{Cp}–C_{strap}$)	11.77°	11°
1,1′:2,2′-Bis(trimethylene)ferrocene **2**		
Fe–ring distance	1.631 Å	1.630 Å
Cp ring tilt angle	10.92°	13.1°
dummy–iron–dummy angle	174.30°	170.01°
ring stagger	0.02°	1.1°
Fe–β–(CH_2) carbon distance	3.262 Å	3.312 Å
Ferrocenediyldiphenylsilane **3**		
Fe–ring distance	1.659 Å	1.65 Å
Cp ring tilt angle	20.21°	19.2°
dummy–iron–dummy angle	165.87°	167.31°
dev of Si from Cp plane	35.56°	40°
Fe···Si distance	2.660 Å	2.636 Å
$C_{Cp}–Si–C_{Cp}$ angle	95.29°	99.1°

The global minimum for $[Fe((CH_3)_4Cp)_2]$ is a structure which is essentially the same as that found in the crystal except for the stagger and methyl group gearing. Bond lengths and angles are reproduced to within a few percent, the structure is partially staggered ($\alpha = 18°$), and the Cp hydrogen atoms are approximately "trans" as observed. The methyl group gearing, however, is not that observed in the X-ray structure. Again, the methyl

Table VIII. Skeletal Force Constants for a Series of Linear Metallocenes

d-config	metallocene	equil distance M-D (Å)	stretch M-D (kcal/mol·Å²)	bend M-D-C (kcal/mol·rad²)	bend D-M-D (kcal/mol·rad²)
d^3	$[V(Cp)_2]$[a,f]	1.928	135	85	50
d^4	$[Cr(Cp)_2]$[a,f]	1.798	150	93	40
d^5	$[Fe(Cp)_2]^+$[b,g]	1.677	205	117	40
d^6	$[Fe(Cp)_2]$	1.649	205	100	40
d^6	$[Co(Cp)_2]^+$[c,g]	1.682	205	100	40
d^6	$[Ru(Cp)_2]$	1.816	205	125	52
d^6	$[Os(Cp)_2]$	1.855	260	130	56
d^7	$[Co(Cp)_2]$[d,g]	1.726	185	45	40
d^8	$[Ni(Cp)_2]$[e,h]	1.817	140	28	40

[a] Gard, E.; Haaland, A.; Novak, D. P.; Seip, R. *J. Organomet. Chem.* **1975**, *88*, 181. [b] Paulus, E. F.; Schäfer, L. *J. Organomet. Chem.* **1978**, *144*, 205. [c] Bockman, T. M.; Kochi, J. K. *J. Am. Chem. Soc.* **1989**, *111*, 4669. [d] Bunder, W.; Weiss, E. *J. Organomet. Chem.* **1975**, *92*, 65. [e] Seiler, P.; Dunitz, J. D. *Acta Crystallogr.* **1980**, *B36*, 2255. [f] Aleksanyan, V. T.; Lokshin, B. V.; Borisov, G. K.; Devyatykh, G. G.; Smirnov, A. S.; Nazarova, R. V.; Koningstein, J. A.; Gächter, B. F. *J. Organomet. Chem.* **1977**, *124*, 293. [g] Stebler, A.; Furrer, A.; Ammeter, J. H. *Inorg. Chem.* **1984**, *23*, 3493. [h] Chhor, K.; Lucazeau, G.; Sourisseau, C. *J. Raman Spectrosc.* **1981**, *11*, 183.

groups are found to adopt the head-to-tail clockwise–anticlockwise conformation.

The minimized structures of $[Ru((CH_3)_5Cp)_2]$, $[Ru((Cl)_5Cp)_2]$, and $[Os((CH_3)_5Cp)_2]$ reproduce the bond and angle parameters of the X-ray structures to within a few percent. The minimized structure of $[Ru((Cl)_5Cp)_2]$ is perfectly eclipsed, as observed in the X-ray structure. For the decamethylmetallocenes we calculate a stagger of 11.16° for ruthenium and a stagger of 10° for the osmium species. In both cases the methyl group gearing is head-to-tail clockwise–anticlockwise as found for the iron analogues. Since neither the methyl group nor the Cp conformations are known for ruthenium or osmium, there is no impetus to comment further on these structures.

9. Strapped Ferrocenes

We found that nearly any reasonable set of force constants for either the skeletal modes or the internal Cp modes could be used to reproduce the structures of linear metallocenes. Thus the preceding examples are not a telling test of the validity of the spectroscopically derived parameters. Perhaps the most stringent way of deciding this question is to examine metallocenes which are highly strained. The three strapped ferrocenes **1–3** have been structurally determined in the solid state.[42–44]

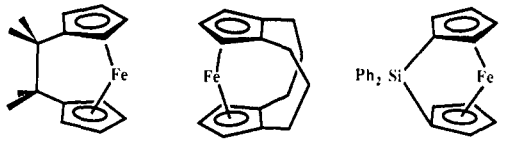

1 2 3

In all three of these molecules, the straps engender considerable strain on both the Cp rings and the metal-Cp framework. Additional force constants associated with the silicon atom were required for **3**. These were derived from reported vibrational spectra of a variety of phenyl- and methylsilanes.[45–49] In all cases the correlation between the calculated and observed frequencies was good. The derived force constants and the equilibrium bond lengths and angles are collected in Table VI. It will be noted that the stretching, bending, and torsion force constants involving the Cp ring are assumed to be the same as those involving a phenyl ring.

In Figure 4 we show the superimposed (rigid-fit) calculated and observed structures of **1–3**. It will be seen that the correspondence between the structures is remarkably good, suggesting that the derived parameters are sufficiently robust to replicate strain in the ferrocenes. Selected bond angles and bond distances for the three calculated and observed structures are given in Table VII. The correspondence is excellent when it is recognized that crystal packing effects are probably sufficient to cause many of the deviations and that the crystal structure of **3** was not refined to high precision.

10. Force Constants for First Row Metallocenes

Although the internal Cp force constants are transferable from one metal to another, this is not the case for the skeletal modes. These latter force constants are dependent on the nature of the metal–Cp bonds. In order to assess this variation, we have determined the force constants associated with the skeletal modes of most of the linear metallocenes of the first transition series. Data are available for the A_{1g}, A_{2u}, E_{1u}, E_{1g}, and E_{1u} skeletal vibrations of $[V(Cp)_2]$, $[Cr(Cp)_2]$, $[Fe(Cp)_2]^+$, $[Co(Cp)_2]^+$, and $[Ni(Cp)_2]$. Only four of the five modes have been identified for $[Co(Cp)_2]$. The 1,5-torsion constant of $[Co(Cp)_2]^+$ can be determined from inelastic neutron scattering.[50] We find a value of 0.7 kcal/mol but the preference for the eclipsed or staggered conformation is not known. There is insufficient data to derive the skeletal force constants of $[Mn(Cp)_2]$.

The skeletal force constants are listed in Table VIII, for which rms deviations for the five observed and calculated frequencies were less than 30 cm^{-1} for the first transition metal series. We have included data for the iron, ruthenium, and osmium species for comparison. In the main, the variations in the force constants from one metal to another are consistent with the current perceptions of the bonding for the various d-configurations. We note that the M–D stretch force constant is the same for Fe(III), Fe(II), Co(III), and Ru(II) but increases for Os(II). Further, the isoelectronic first row metals Fe(II) and Co(III) have identical force constants.

11. Discussion

One of the daunting prospects of developing molecular mechanics force fields for organometallic species is the enormous variety of structures, stereochemistries, and metals that exist. The present study may provide a useful foundation from which other organometallic parameters may be derived. Although we have attempted to derive the force field for linear metallocenes with a tolerable degree of rigor, the van der Waals parameters for the metals could be refined rather than adopting the generic parameters used here. Similarly, the electrostatic calculations need to be quantified better. Even so, the force field derived here provides an excellent molecular model for linear metallocenes.

We have shown that the internal Cp force constants are transferable from metal to metal to a very good approximation. Force field calculations would be simpler and more general were

(42) Laing, M. B.; Trueblood, K. N. *Acta Crystallogr.* **1965**, *19*, 373.
(43) Hillman, M.; Austin, J. D. *Organometallics* **1987**, *6*, 1737.
(44) Stoekli-Evans, H.; Osborne, A. G.; Whiteley, R. H. *Helv. Chim. Acta* **1976**, *59*, 2402.
(45) Smith, A. L. *Spectrochim. Acta* **1968**, *24A*, 695.
(46) Smith, A. L. *Spectrochim. Acta* **1967**, *23A*, 1075.
(47) Murata, H.; Kawai, K. *J. Chem. Phys.* **1955**, *23*, 2451.
(48) Kriegsmann, H.; Schowtka, K. H. *Z. Physik. Chem.* **1958**, *209*, 261.
(49) Shimizu, K.; Murata, H. *J. Mol. Spectrosc.* **1960**, *5*, 44.
(50) Sourisseau, C.; Mathey, Y.; Poinsignon, C. *Chem. Phys.* **1982**, *71*, 257.

it possible to take a set of generic skeletal force constants and use these for deriving structures with acceptable accuracy. As we have shown, the skeletal force constants are not generally transferable. If, however, one only wishes to obtain good structures of linear metallocenes, these force constants can be obtained for the metals in Table VIII by simply using those of ferrocene as a generic set, provided the correct equilibrium bond lengths and angles are used. This will probably apply even for somewhat strained linear metallocenes.

Acknowledgment. This work was supported by grants from the National Institutes of Health.

Homologation of Olefins with Methane on Transition Metals

Tijs Koerts,[†] Piet A. Leclercq,[‡] and Rutger A. van Santen*,[†]

Contribution from the Schuit Institute of Catalysis, Department of Inorganic Chemistry and Catalysis and Laboratory of Instrumental Analysis, Eindhoven University of Technology, P.O. Box 513, 5600 MB Eindhoven, The Netherlands. *Received December 27, 1991*

Abstract: Alkylation of olefins using methane has been realized on transition metal catalysts. The main problem is to get methane dissociatively adsorbed together with an olefin. This is due to the difficult activation of the strong tetrahedral C-H bonds of methane. To react methane with an olefin, a reaction sequence is used consisting of three steps. First methane is dissociatively adsorbed between 600 and 800 K on a reduced transition metal catalyst. After cooling, an olefin is coadsorbed at a temperature between 300 and 400 K. Upon subsequent hydrogenation carbon–carbon bond formation occurs. The mechanism appears to be related to that occurring in the Fischer–Tropsch reaction. After hydrogenation the reaction cycle can be repeated. Methane addition to ethene, propene, and acetylene is demonstrated to occur using silica-supported ruthenium and cobalt catalysts. With $^{13}CH_4$ it was shown that propane and butane are formed both by self-homologation of ethene and propene, respectively, as well as by methane incorporation. Carbon scrambling according to the metathesis reaction is very slow.

Introduction

Methane homologation is of interest because of the many reactions that proceed via CH activation or carbon–carbon bond formation. Selective methane activation is difficult owing to the strong tetrahedral C-H bonds that lack polarity, and the ease of consecutive reactions of the resulting CH_x groups.

Many different approaches have been developed in the activation of C-H bonds in alkanes, using organo-metal systems,[1-4] heterogeneous catalysts,[5-7] gas-phase metal ions,[8,9] homogeneous catalysis,[10,11] or biochemical systems.[12] On transition metals the mechanism of dissociative alkane adsorption has been extensively studied on single crystals.[13-18] The activity for metal films to activate methane at temperatures starting at 400 K was demonstrated by Bond[19] and Frennet[20] from the methane–deuterium exchange reaction. Dissociative methane adsorption on transition metal catalysts has a relative low activation energy (25–60 kJ/mol).[21,22,56] However, to realize reasonable sticking coefficients for chemisorption, methane has to be activated.[23-25] Dissociative methane adsorption at high temperature results mainly in unreactive coke formation.[26,27] At mild conditions alkanes can be activated selectively with organo-metal complexes.[1-3,28] In such a reaction the metal center (M) of the complex is able to interact with an alkane (R-H) and can finally insert into the C-H bond according to R-H + M → R-H···M → R-M-H.

Recently it has been found that hydrocarbons can be formed when methane is activated on a Ni single crystal[2,30] or on supported metal catalysts.[31-33] We have shown previously[34,56] that when methane is activated thermally under mild conditions, a surface C_1 intermediate can be generated that is able to produce C_2^+ hydrocarbons upon hydrogenation. This occurs according to a Fischer–Tropsch synthesis type mechanism for carbon–carbon bond formation.[35] O'Donohoe showed that the direct homologation of alkanes to a higher homologue is possible on tungsten catalysts.[36,37] Also oxidative methylation of propene to butene has been reported[38,39] on rare earth oxides.

Alkylation of olefins with methane to an alkane with one extra carbon atom is thermodynamically possible below 500 K in one step.[40] This reaction has been found to occur using superacids as catalysts.[41] Syskin and Mayer[42] converted methane–ethene

[†] Schuit Institute of Catalysis.
[‡] Laboratory of Instrumental Analysis.

(1) Crabtree, R. H. *Chem. Rev.* **1985**, *85*, 245.
(2) Bergman, R. G. *Science* **1984**, *223*, 4639.
(3) Shilov, A. E. *Sov. Sci. Rev. Sect. B: Chem. Rev.* **1982**, *B4*, 71.
(4) Crabtree, R. H.; Holt, E. M.; Lavin, M.; Morekous, S. M. *Inorg. Chem.* **1985**, *24*, 1986.
(5) Baerns, M. *Nachr. Chem. Tech. Lab.* **1985**, *33*, 292.
(6) Pitchai; Klier, *Catal. Rev.-Sci. Eng.* **1968**, *28*, 13.
(7) Anderson, J. R. *Appl. Catal.* **1989**, *47*, 177.
(8) Irikura, K. K.; Beauchamp, J. L. *J. Am. Chem. Soc.* **1991**, *113*, 2769.
(9) Schwarz, H. *Angew. Chem.* **1991**, *103*, 837.
(10) Olah, G. A. *Top. Curr. Chem.* **1979**, *80*, 17.
(11) Olah, G. A.; Parker, D. G.; Yoneda, N. *Angew. Chem.* **1978**, *90*, 962.
(12) Patel, R. N.; Hou, C. T.; Laskin, A. I.; Felix, A. *J. Appl. Biochem.* **1982**, *4*, 175.
(13) Hamza, A. V.; Madix, R. J. *Surf. Sci.* **1987**, *179*, 25.
(14) Szuromi, P. D.; Weinberg, W. H. *Surf. Sci.* **1985**, *149*, 226.
(15) Salmeron, M.; Somorjai, G. A. *Surf. Sci.* **1981**, *85*, 3835.
(16) Arumainayagam, C. R.; McMaster, M. C.; Schoofs, G. R.; Madix, R. J. *Surf. Sci.* **1989**, *222*, 213.
(17) Trevor, D. J.; Cox, D. M.; Kaldor, A. *J. Am. Chem. Soc.* **1990**, *112*, 3742.
(18) Brass, S. G.; Ehrlich, G. *Phys. Rev. Lett.* **1986**, *57*, 2532.
(19) Bond, G. C. In *Catalysis by Metals*; Academic Press: New York, 1962.
(20) Frennet, A. *Catal. Rev.-Sci. Eng.* **1974**, *10*, 37.
(21) Tavares, M. T.; Bernardo, C. A.; Alstrup, I.; Rostrup-Nielson, J. R. *J. Catal.* **1986**, *100*, 545.
(22) Kuijpers, E. G. M.; Jansen, J. W.; Van Dillen, A. J.; Geus, J. W. *Catal.* **1981**, *72*, 75.
(23) Schwarz, H. *Acc. Chem. Res.* **1989**, *22*, 282.
(24) Kay, B. D.; Coltrin, M. E. *Surf. Sci.* **1988**, *198*, L375.
(25) Rettner, C. T.; Pfnür, H. E.; Auerbach, D. J. *Phys. Rev. Lett.* **1985**, *54*, 2716.
(26) Sault, A. G.; Goodman, D. W. *Adv. Chem. Phys.* **1989**, *76*, 153.
(27) Van Der Zwet, G. P.; Hendriks, P. A. J. M.; Van Santen, R. A. *Catal. Today* **1989**, *4*, 365.
(28) Chatt, J.; Davidson, J. M. *J. Chem. Soc.* **1965**, 843.
(29) Yang, Q. Y.; Johnson, A. D.; Maynard, K. J.; Ceyer, S. T. *J. Am. Chem. Soc.* **1989**, *111*, 8748.
(30) Ceyer, S. T. *Science* **1990**, *249*, 133.

0002-7863/92/1514-7272$03.00/0